

POWER TRANSISTOR AND PHOTODIODE AS A SOLAR CELL DEVICE

UHUEGBU C.C⁺. AND AYARA W. A.

DEPARTMENT OF PHYSICS
COVENANT UNIVERSITY, OTA
OGUN STATE NIGERIA

ABSTRACT

Novel solar panel using BPW41N Photodiode have been developed. The panel produced current of 714 μ A at 6.17V and 375 μ A at 8.60V using type A and B respectively. The combination of type A and B produced current of 395 μ A at 13.80V which is a 5.45mW solar panel.

Keywords: solar panel, photodiode, transistors, current, voltage

INTRODUCTION:

One of the earliest recorded observations of photovoltaic effect was made by Becquerel in 1939 while working with electrolytic cells. This was followed by the discovery of Selenium and the preparation of element Silicon in 1817 and 1823 respectively by [1]-[4].

Further research of Adams and Day resulted in the discovery of the photovoltaic properties of Selenium in 1877 and the development of Selenium solar cell in 1883 by [5]-[8].

The research efforts on the photovoltaic properties of Silicon based cells reached a turning point in the late 1950's when American Scientists successfully achieved solar energy conversion using p-n junction semiconductor. The p-n junction semiconductor was made by the refinement of impurity diffusion methods of p-n junction formation [9].

The production of cost effective and efficient solar cells from monocrystalline and polycrystalline semiconductor. The best commercially available cells today are made from monocrystalline Silicon with efficiencies of around 15% [3].

The cost of solar modules is far outside the reach of the common man in Nigeria for instance, a 6 –watt module cost as much as N12, 000. This cost is because the manufacturing process of the solar cells involves sophisticated technology. For instance it involves the production and processing of Silicon wafers with a thickness in the range of 0.25mm to 0.35 mm [10]. In an inert atmosphere and under carefully controlled conditions such that the required high material quality can be achieved. Solar cell is precisely a p-n junction designed and normally connected to operate in the zero bias mode which is the photovoltaic mode [11], [12].

In a photovoltaic process energy is obtained by absorbing photons of light. A photon is a material phenomenon which exhibits a wave particle characteristic. It is practically a packet of light and has an amount of energy **E** that is a function of frequency **f** and wavelength λ [13].

$$E = hf = \frac{hc}{\lambda} \quad 1$$

Where **h** is Planck's constant **f** is the frequency **c** is the velocity of light, λ wavelength

$$E = \frac{1.24eV}{\lambda (\mu m)} \quad 2$$

A semiconductor of energy gap E_g will absorb photon with energy E if and only if E is greater than E_g . If the photon is less than the semiconductor energy gap, it will not be absorbed [7].

The energy gap of a semiconductor decreases with increasing temperature [9]. The electron- hole pair generated in a semiconductor under illumination have only finite lifetime, T after which they will combine.

This depend on the electron and hole densities and hence a function of the doping densities in a doped semiconductor.

The idealized equivalent circuit of the photovoltaic cell consists of constant current source I_{ph} , saturated current I_s

$$I_L = I_s - I_{ph} \tag{3}$$

where $I_s = I_0(e^{ev/kt} - 1) - I_{ph}$ is the diode saturation current, I_{ph} is the carrier by solar radiation [9] and is called the photocurrent.

It was shown that by [14] that photocurrent is a function of light intensity. Design and junction reflectively is given by

$$J_{ph} = J_n + J_p + J_{dr} \tag{5}$$

Where J_p is the current density due to the electron in the P-side of the junction J_n is the current density due to the holes in n-side of the junction.

J_{dr} is the current density due to the photo carrier in the depletion region.

$$I = I_0(e^{ev/kt} - 1) - I_{ph}$$

$$V_{OC} = \frac{KT}{q} \ln(I_L/I_0 + 1) \tag{6}$$

The photo current is proportional to incident light intensity while V_{oc} has a logarithmic relationship with the photocurrent I_{ph} .

Photovoltaic cells theory of operation

A photovoltaic process basically involves:

- i The absorption of light photons for the creation of electron - hole pairs within the bulk of the material device.
- ii The separation of the electron - hole pairs so generated to prevent recombination and self annihilation.
- iii The high mobility of the separated charge carriers that enables them to move freely through the device to the external contacts and hence through an external load to furnished away desired power.

Solar cells are solar photovoltaic converters. A solar cell is a metal-semi-conductor contact device. The incident photons of solar radiation can lift electrons from the valency band to the conduction band. This is possible when $E_g \leq hf$, E_g is the band gap equal to $(E_c - E_v)$ and hf is the photon energy. E_c is conduction band energy and E_v is the valency band energy. Photons with energy $hf < E_g$ do not make any contribution $F_g = E_g$ is therefore threshold frequency for photon electron emission. If F_g can be lowered, more electrons will be energized enough to be raised from valency band to conduction band resulting in an increase in the efficiency of the solar cell.

Solar cell models by the real model of the solar cell, it is possible to predict the quantity of power which the cell can deliver and by studying the ideal model, it is possible to locate necessary improvement with a view to produce more efficient cells. An ideal solar cell is in parallel with constant current source in figure 1 resulting from the excitation of electrons in excess and drift of the excess across the schotlky barrier. The current-voltage characteristics of the solar cell is given by

$I = I_0(e^{ev/kt} - 1) - I_L$ where I_0 is the reverse saturation current and I_L is the constant current source.

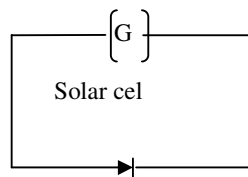


Fig. 1 ideal solar cell.

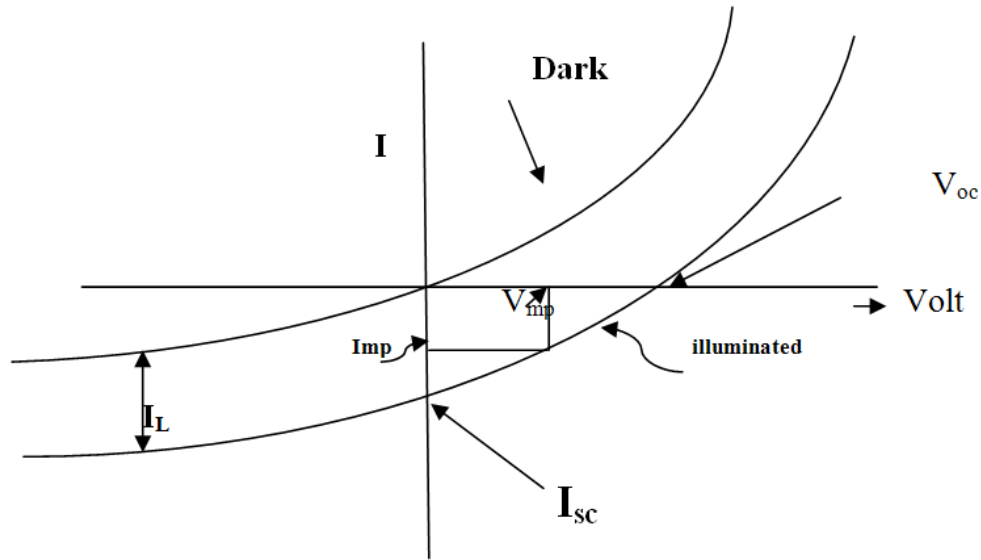


Fig.2 current – Voltage characteristics

Three parameters are usually used to characterize solar cell output. One of these is the short-circuit current, I_{sc} . Ideally, this is equal to the light generated current I_L . A second parameter is the open-circuit voltage V_{oc} . Setting I to zero in figure 2.

$$I = I_0 (e^{qv/kt} - 1) - I_L$$

Gives,

$$V_{oc} = \frac{KT}{q} \ln(I_L/I_0 + 1) \approx \frac{KT}{q} \ln(I_L/I_0)S \tag{7}$$

Where V_{oc} is the open circuit voltage. V_{oc} is determined by the properties of semi-conductor by virtue of its dependence on I_0 . The power output at any operating point in the fourth quadrant in figure 2 is equal to the area of the rectangle in figure 2. one particular operating point (V_{mp} , I_{mp}) will maximize this power output. The third parameter is the fill factor (FF) which is given as

$$FF = V_{mp} I_{mp} / V_{oc} I_{oc} \tag{8}$$

It is a measure of how “square” in shape the output characteristics are. It is a function only of the open-circuit voltage V_{oc} . It has a value in the range of 0.7 to 0.85 and it is given by the relation,

$$FF = V_{oc} - \ln(V_{oc} + 0.72)/V_{oc} + 1 \tag{9}$$

Optical efficiency is defined as the fractional solar radiation reaching the receiver and absorbed. The energy conversion efficiency η is given by

$$\eta = V_{mp} I_{mp} / P_{in} = V_{oc} I_{mp} FF / P_{in} \tag{10}$$

Where P_{in} is the total power in the light incident on the cell. Saturation current density as a function of band gap is given by

$$I_0 = 1.5 \times 10^5 e^{(-E_g/KT)} \text{ A/cm}^2 \tag{11}$$

The short -circuit current of solar cell is not strongly temperature-dependent. It tends to increase slightly with increasing temperature. This is attributed to increase light absorption, since semi-conductor band gaps generally decrease with temperature.

$$I_{sc} = I_0 (e^{qv/KT} - 1) \tag{12}$$

Neglecting the small negative term

$$I_{sc} = A T^\gamma e^{-E_g/KT} e^{qvoc/KT} \tag{13}$$

Where $I_0 = AT^\gamma e^{-E_{go}/KT}$

A is independent of temperature, E_{go} is the linearly extrapolated band gap of the semiconductor at zero temperature. Making up the cell γ includes the temperature dependence of the remaining parameter determining I_0 . Its value generally lies in the range of 1 to 4 with $V_{go} = E_{go}/q$. Differentiating we have

$$dI_{sc}/dT = A\gamma T^{\gamma-1} e^{q((v_{oc}-v_{go})/KT)} + AT^\gamma q/KT dV_{oc}/dT - ((v_{oc}-v_{go})/T) - e^{q((v_{oc}-v_{go})/KT)} \quad 14$$

neglecting dI_{sc}/dT in comparison with more significant terms, gives

$$dV_{oc}/dT = -v_{go} - v_{oc} + \gamma(KT/q)/T \quad 15$$

This predicts an approximately linear decrease in V_{oc} with increasing temperature values for silicon, $V_{go}=12V$, $V_{oc} = 0.6V$, $\gamma = 3$, $T = 300K$

$$dV_{oc} / dT = -12-0.6+0.078 / 300 \text{ V/C} = -2.3mV/^{\circ}C$$

This agrees with experimental results. Hence for Silicon V_{oc} decreases by 0.4% per $^{\circ}C$. The fill factor decreased with variation that of V_{oc} . This causes the power output and efficiency to decrease by 0.4 to 0.5% per $^{\circ}C$.

Methodology

Basically two semiconductor devices were used in carrying out this work; power transistors 2N3055 and photodiodes BPW41N. The 2N3055 is a silicon epitaxial-Base planner NPN transistor that is mounted in a TO -3 metal case. It is very well intended for power switching circuit, series and shunt regulators, output stages and for high fidelity amplifiers [15].

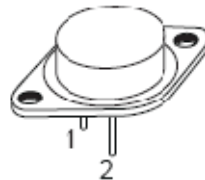


Fig. 3: Physical diagram of 2N3055

The BPW41N is a high speed and high sensitive PIN photodiode enclosed in a flat side view plastic package. Its package is an IR filter, that is spectrally matched to GaAs or GaAs on GaAlAs IR emitter ($\lambda=950nm$). It large area combined with the flat case gives it a high sensitivity at a wide viewing angle [16].

Below is a diagram showing how the device looks.

The photodiodes are of two types (stock) although they have the same part number “BPW41N”. Hence the photodiode is divided into type A (stock A) and type B (stock B).



Fig. 4: Physical diagram of BPW41N

The following materials, pliers, bench vice, breadboard, digital multimeter, Analog meter (micro ammeter and voltmeter), thermometer and connecting wire were used in this work.

The metal case covering the 2N3055 chips were opened using a plier while using the bench vice to securely hold the transistor in place.

This was followed carefully by cleaning the opened surface with cotton wool soaked with alcohol, to clear off any dust particle that may have settled on the chip in the course of opening.

The arrays of transistors were connected electrically in parallel and series.

All the base terminals were connected to point A, while the entire emitter terminals were connected to point B. Between the point A and B a voltmeter and a micro ammeter were connected to monitor the change in voltage and current respectively as the circuit is exposed to sun light. Note that the collector terminal is left unconnected in the circuit.

In the series connection, the emitter of one transistor is connected to the base terminal of the next transistor leaving out the base terminal of the first transistor and the emitter terminal of the last transistor as the end terminals.

Connecting a voltmeter and a micro ammeter across point A and B as shown in fig.2, monitor the change in voltage and current with the change in the intensity of sun light radiation

The photodiode BPW41N was connected in series arrangement. The cathode of the first photodiode was connected to the anode of the next photodiode. This process was followed until the anode of the first photodiode and the cathode of the last photodiode were left as the final output terminal where the voltmeter and the micro ammeter were connected to monitor the variation in the output voltage and current.

RESULT

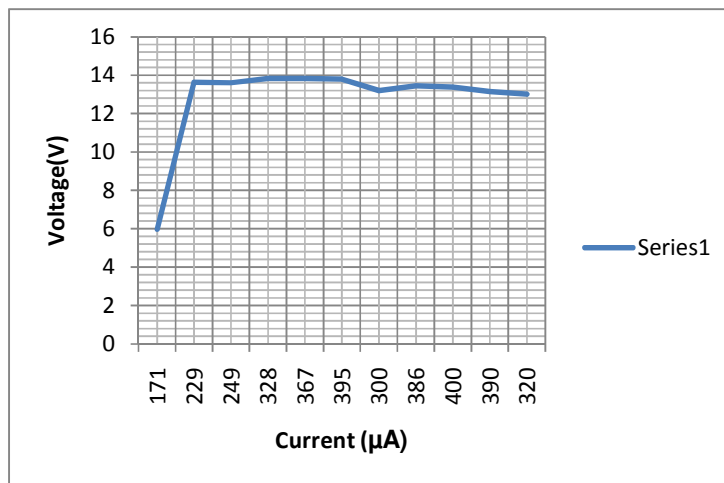


Fig. 5 graph of voltage verse current

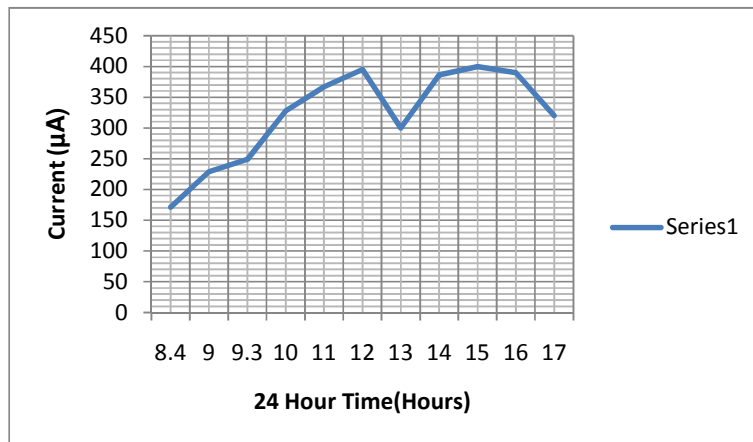


Fig.6. graph of current verse time

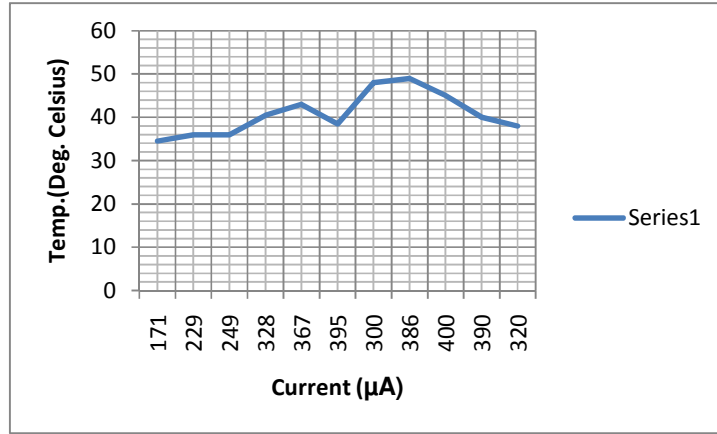


Fig. 7 graph of temperature verse current

Fig. 5 to fig.7 represent the result for the combination of type A and B of BPW41N photodiodes.

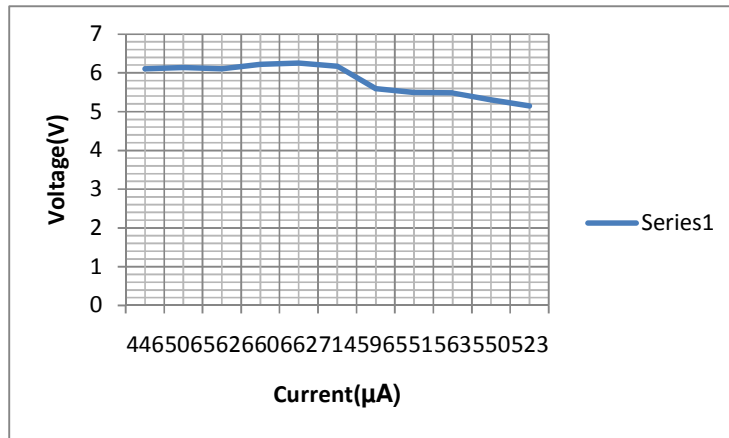


Fig.8 graph of voltage verse current

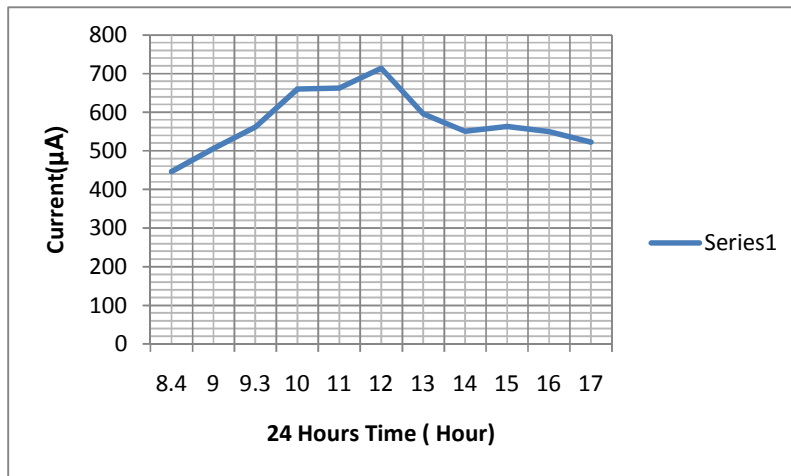


Fig.9 graph of current verse time

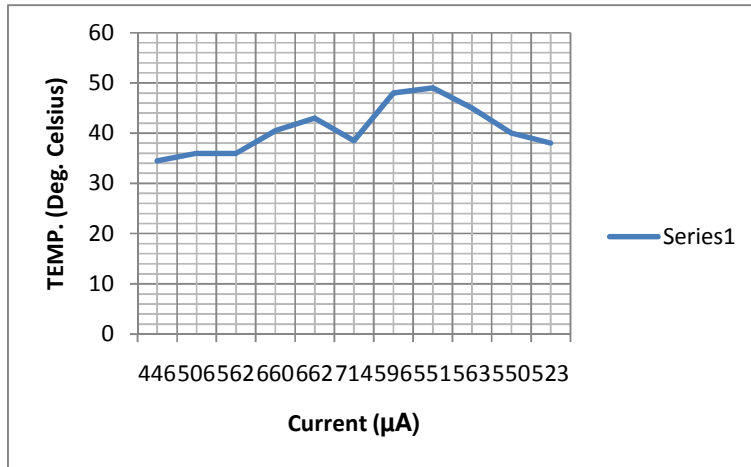


Fig.10. graph of temperature verse current

Fig.8 to fig.10 represent result for type A of BPW41N photodiode.

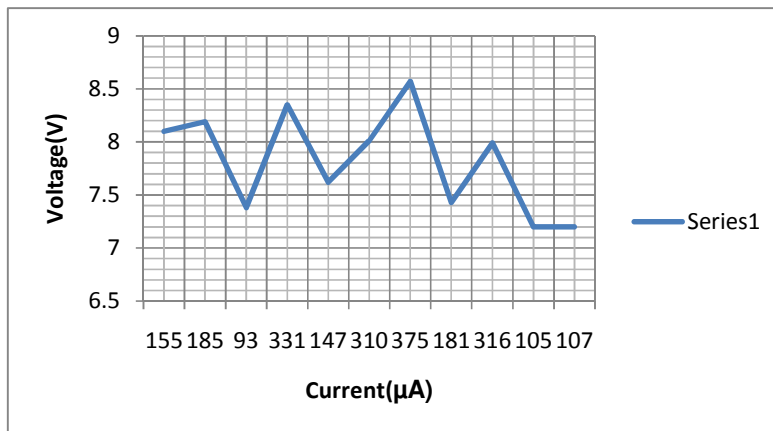


Fig.11. graph of voltage verse current

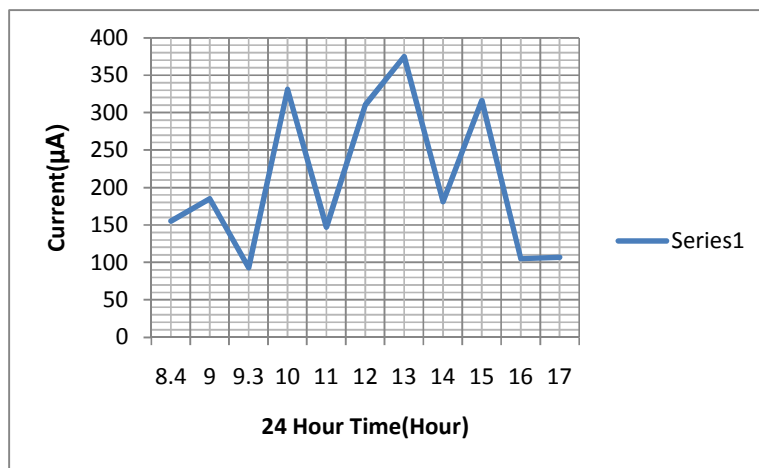


Fig.12. graph of current verse time

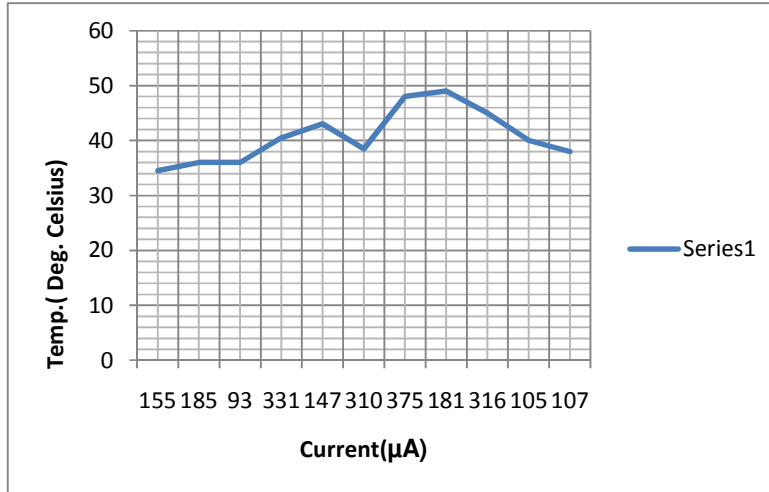


Fig.13. graph temperature verse current

Fig. 11 to 13 represent results for type B of BPW41N photodiodes.

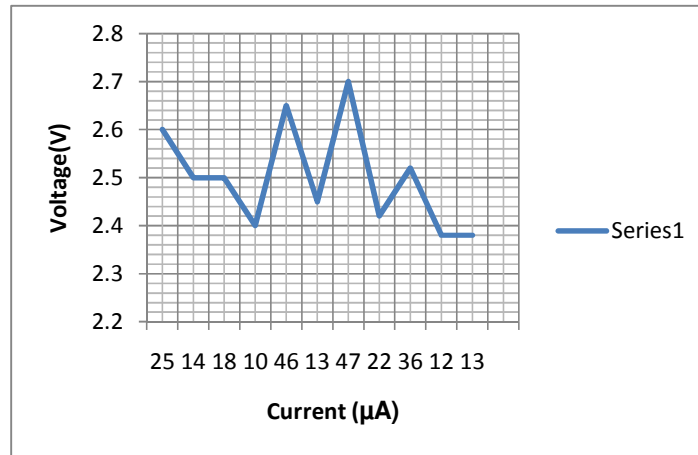


Fig. 14 graph of voltage verse current

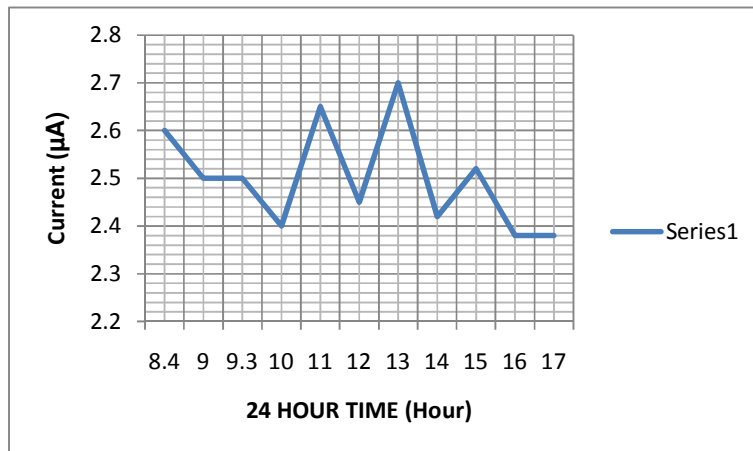


Fig. 15.graph of current verse time

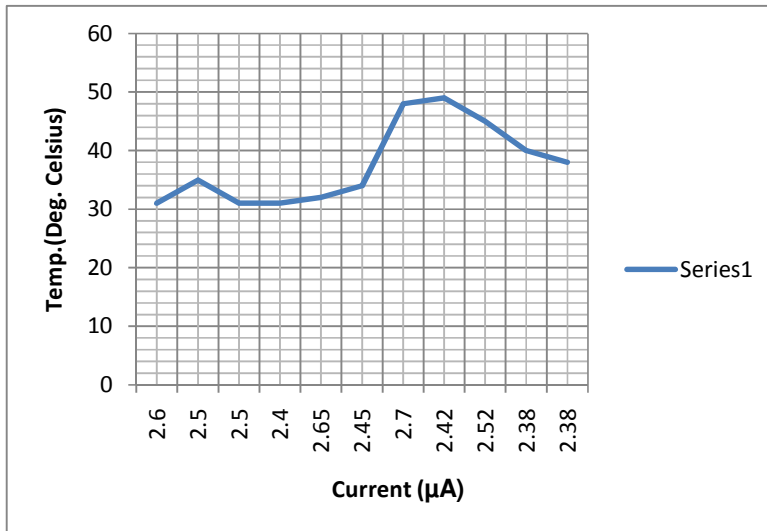


Fig. 16 graph of temperature verse current

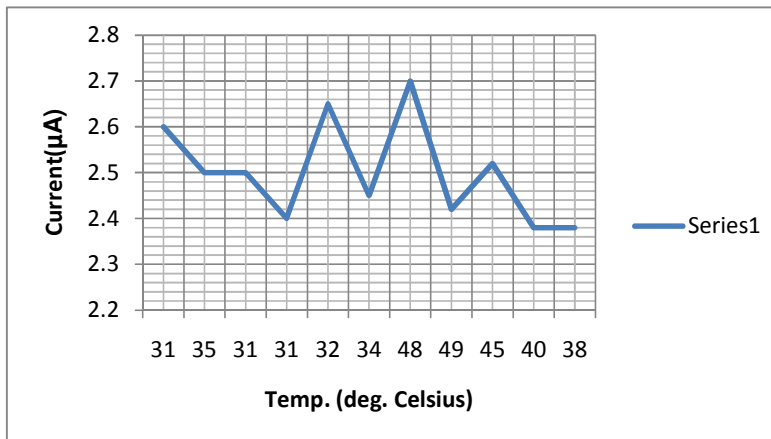


Fig.17. Graph of temperature verse current

Fig. 14 to 17 represents the results for SERIES connection of the power transistor 2N3055.

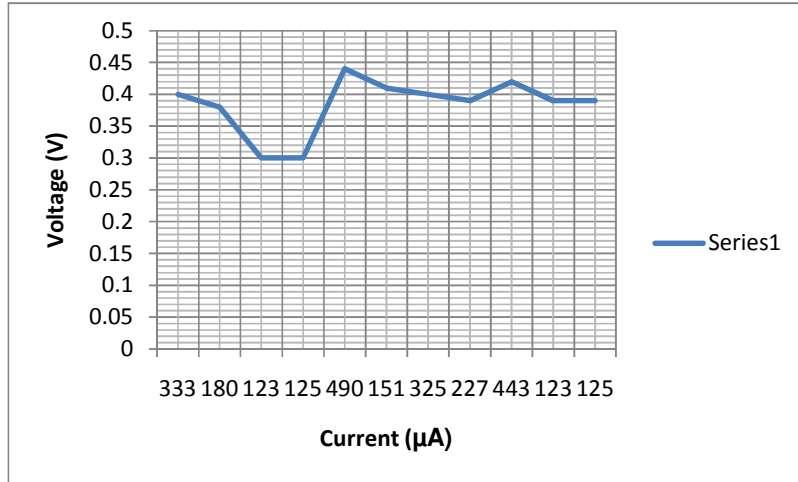


Fig. 18. Graph of voltage verse current

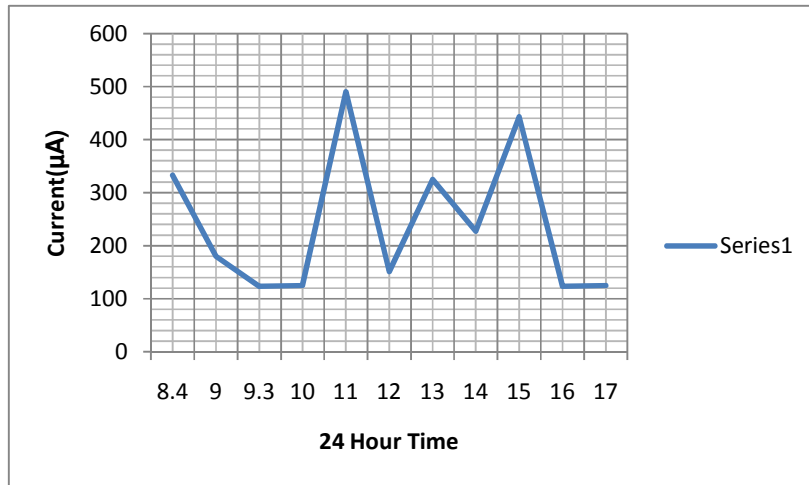


Fig. 19 graph of current verse time

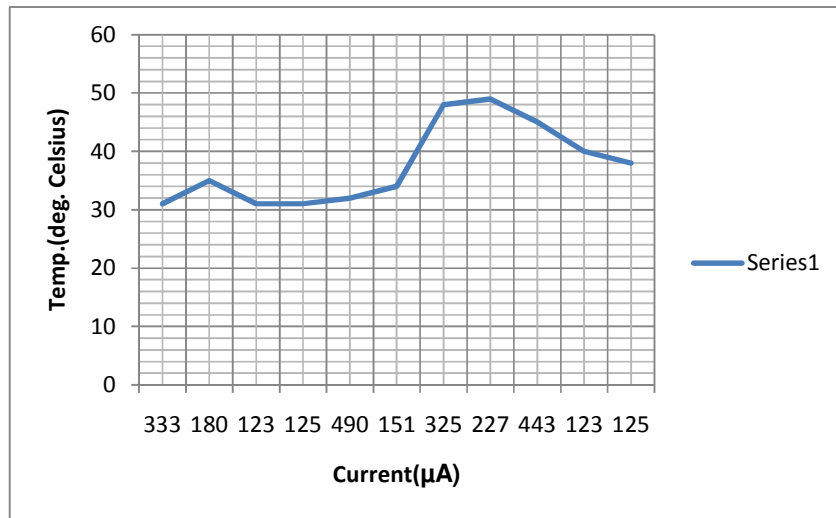


Fig. 20 graph of temperature verse current

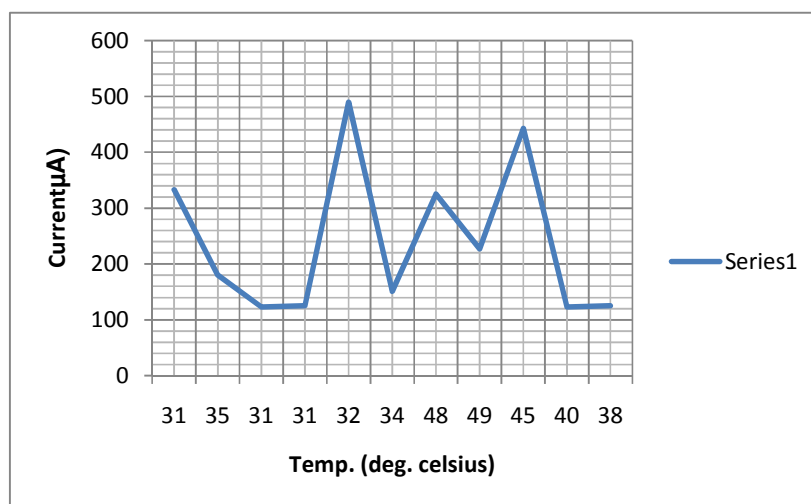


Fig. 21 graph of current verse temperature

Figs. 18 to 21 represent the results for PARALLEL connection of the power transistor 2N3055.

DISCUSSION

Figures 5, 8, 11, 14, and 18 are graphical representations showing the relationship between voltage and current produced when BPW41N photodiode and 2N3055 power transistors are respectively exposed to sunlight.

It was observed from fig.5 and 8 graphs of voltage verses current that the combination of Type A and B of BPW41N photodiode generated a maximum of 395µA at 13.80V compared to 714µA at 6.17V generated by Type A and 375µA at 8.60V for Type B.

Although Type A and B is a combination of the two different stocks of BPW41N photodiode, it generated less amount of current at a voltage higher than those of Type A and B separately connected.

Type A photodiode of BPW41N generated greater amount of current compared with the others. This implies that with large quantity of type A BPW41N, more current are likely to be generated.

From figs. 14 and 18, greater amount of fluctuations were observed. The voltage generated was between 0.40V and 2.70V with current of 490 µA. This is low compared with Type A of BPW41N photodiode.

Figures 7, 10, and 13 show the graphs of temperature against current for the BPW41N photodiode. It was observed that maximum current generated by type A, type B and combination of types A and B for the BPW41N occurred at temperature below 40°C. This implies that current generation by BPW41N is not dependent on high temperature.

From figures 16 and 20 current was generated by 2N3055 at temperature close to 50°C. This current is less compared to that generated by BPW41N.

Using BPW41N and 2N3055, maximum current was generated between 12noon and 1.00pm of each day indicating that at these stated time maximum solar radiation is being received.

The BPW41N generated more current than the 2N3055 transistor because BPW41N is a PIN photodiode which has a wide depletion region called the intrinsic region width that enhances the generation of more photocurrent and BPW41N is designed in such a way that it has a high speed of response [17], hence it has prompt photocurrent generation.

CONCLUSION

We have successfully developed a novel solar panel using BPW41N photodiode. The panel produced 714 μ A at 6.17V and 375 μ A at 8.60V with type A and B of the BWW41N respectively. The combination of type A and B produced current of 395 μ A at 13.80V, which is 5.45mW solar panel.

We conclude that more current could be produced if the number of the photodiodes are increased.

The cost of the prototype is ₦7, 350. It is estimated that a 40W prototype panel will cost ₦175,000. Due to its high speed of response, at maximum solar radiation greater amount of photocurrent will be generated.

REFERENCES

- [1] Megbowon, I.O and Alowolou, K.E (1984). The photovoltaic properties of a silicon power Transistor, Bsc Thesis FUTA Nigeria
- [2] Cody, A, B.G .Books and B. Abeles (1982), Optical absorption above the optical gap of Amorphous Silicon hydride, Solar Energy Material Vol.8,231-240
- [3] Barter, A (1984) Semiconductor and Electronic devices 2nd Edition
- [4] Charise, H.K Jr(1984) Solar Photovoltaic Energy System John Hopkins University Maryland.
- [5] Green Peace (2001) Solar generation for the European PV industries Assoc.
- [6] Blatt, J. (1968) Physics of electronic Conduction in Solids McGraw Hills Books Company New York.
- [7] Chopra L. and S.R. Das (1983), Thin film solar cells, Plenum Press New York.
- [8] Van Campen, B. and Guidi D (2000), Solar Photovoltaic for sustainable Agriculture and rural development. FAO United Nations, Rome, Italy.
- [9] Sze S.M (1985) Semiconductor Devices, Physics and Technology. John Wiley & Sons.
- [10] Okujagu, C.U and C.E. Okeke (1998), Growth and Characterization of some spectrally selective halide and chalcogenide thin film, Nigerian Journal of Renewable Energy. Vol.6. No.1, 52-61.
- [11] Pramanik, P., S. Bhattacharya and P.K Basu (1987), Solution Growth technique for the deposition of Cobalt Solenoid thin films; Thin Solid films Vol. 149, 181-184.
- [12] Varkey, A.J (1989), Chemically deposited thin films Solar Energy Applications. Nigeria Journal of Solar Energy Vol. 6
- [13] Rai G.D (2004), Solar Energy Utilization. Ramesh Chander Khanna Publishers, Delhi India.
- [14] Calvert, J.M and M.A.H. McCausland (1982) Electronics, John Wiley & Sons New York.
- [15] ON Semiconductor (2001) Rev.3 March publication, order number 2N3055 A/D
- [16] www.vishay.com (1999) Rev.2 20 May, Document number 81522
- [17] Donald A. Naemen (2003), Semiconductor Physics and Devices Basic Principle, 3rd edition 634- 649